Electronic Supplementary Information for:

Graphene oxide beads for fast cleanup of hazardous chemicals

Chenlu Bao, Shuguang Bi, He Zhang, Jinliang Zhao, Pengfei Wang, Chee Yoon Yue, and Jinglei Yang*

Dr. C. L. Bao, Dr. S. G. Bi, Dr. H. Zhang, Mr. J. L. Zhao, Dr. P. F. Wang, Prof. C. Y. Yue, Prof. J. L. Yang. School of Mechanical and Aerospace Engineering, Nanyang Technological University, 50 Nanyang Avenue, Singapore, 639798, Singapore.

Mr. J. L. Zhao. Interdisciplinary Graduate School, Nanyang Technological University, 50 Nanyang Avenue, Singapore. 639798, Singapore

Dr. P.F. Wang. CAS Key Laboratory of Mechanical Behavior and Design of Materials, and Department of Modern Mechanics, University of Science and Technology of China, Hefei, 230026, PR China

Prof. J.L. Yang. Department of Mechanical and Aerospace Engineering, The Hong Kong University of Science and Technology, Clear Water Bay, Kowloon, Hong Kong, China. E-mail:maeyang@ust.hk

This world file contains:

Supplementary text

Fig. S1–S16

Supplementary text

1. Influence of extruding parameters on the formation of GO beads

The extruding parameters include the size of the channel in nozzle, the extruding speed of GO/water dispersions, and the distance between nozzle and the surface of coagulating bath (*h* in Fig. 1d, and Fig. S2, g–i).

The size of the channel in the nozzle directly affects the size of GO beads (Fig. S2e). The nozzle provides flowing channels for GO/water disperisons and help to form GO/water droplets, which are the precursors of GO beads. When using a plastic dropper (inner diameter 7 mm, "1" in Fig. S2e) as the nozzle, the diameter of the obtained GO beads is about 10 mm. When using a needle (inner diameter 1 mm, "3" in Fig. S2e), the diameter of the obtained GO beads is about 3 mm.

Extruding speed of GO/water dispersion is the key to achieve bead-like spheroid morphology. Low speed usually leads to spheroid beads, while high extruding speed usually results in fibers-like structures. Fig. S2f, g, h and i show an example that uses 1 mm needle as nozzle. When the extruding speed is higher than 10 ml/min, GO/water dispersions flow continuously, and finally form GO fibers (Fig. S2f). When the extruding speed is 4 ml/min or smaller, GO/water dispersions form droplets which drip into coagulating bath one by one and result in GO beads (Fig. S2h). In addition, when the extruding speed lies in the range of 5–9 ml/min, GO/water droplets usually drip fast and hit the earlier ones when immersing into coagulating bath, and hence is not preferred.

Nozzle-bath distance, the *h*, directly influences the formation of GO beads (Fig. S2, g–i). If the *h* is too large, GO/water droplets are flattened or deformed due to the high impact when they hit the surface of coagulating bath (Fig. S2g). If the *h* is too small, GO/water droplets cannot immerse into coagulating bath but float on the bath (Fig. S2i), probably because the potential energy of the droplets is not large enough to overcome the surface tension of coagulating bath. Only when the *h* is in a suitable range, GO/water droplets can immerse into coagulating bath with spheroid morphology (Fig. S2h). In our experiments, the optimized *h* usually lies in the range from 5 mm to 30 mm.

It should be noted that the optimized extruding parameters are influenced by many factors. The preferred size of the channels in the nozzle is, to some degree, related to the viscosity of GO/water dispersions. Dispersions with low viscosity usually prefer small channels, while highly viscous dispersions can be extruded using the nozzle with large channels. The Optimized extruding speed depends on the total size of the channels in the nozzle. For instance, when using a needle, which has only one channel, as the nozzle, the extruding speed should be low; when using a shower nozzle, which has many channels, as the nozzle, then the extruding speed can be high. The h is determined by the density and surface tension of coagulating bath, and is also related to the concentration of GO/water disperisons. Thus, in every preparation of GO beads, these parameters need to be adjusted according to the real conditions.

2. Influence of post-treatments on the structure and properties of GO beads

The post-treatments of GO beads, including the drying operation and reduction process, can improve the structure, properties and applications of GO beads.

The substances in wet GO beads are mostly water. If dried in a drying oven or vacuum oven, or dried just in a fume hood, the wet beads shrunk to small particles due to the loss of water (Fig. S11). Therefore, freeze-drying is preferred so as to keep the spheroid morphology.

The reduction process can be chemical reduction or thermal reduction. The later one is preferred due to its high convenience, particularly when processing GO beads at large scale. Here, the GO beads coagulated using CTAB or PEI are dried by freeze drying and then heated in a drying oven at 150 ^{o}C or 300 ^{o}C (Table S1). The surface of reduced GO beads turned to black or silvery (Fig. S5 and S6), indicating the reduction of GO. In the heat and reduction process, gases are released and erode the shells of GO beads. GO beads coagulated for 1 h or 5 h (CTAB-1 h-300 ^{o}C, CTAB-5 h-300 ^{o}C and PEI-1 h-300 ^{o}C) are mostly broken or disassembled after the heat treatments (Table S1, Fig. S5 and S6), implying the fragility of the shells are weak. In contrast, GO beads coagulated for 24 h are strong enough to suffer the impact of gases, implying the coagulation process strengthens the shells of beads. In our experiments, the reduction at 150 ^{o}C is preferred because, firstly, it does not destroy the structure of GO beads, and, secondly, it retains the amphipathicity of GO beads.

Supplementary Figures

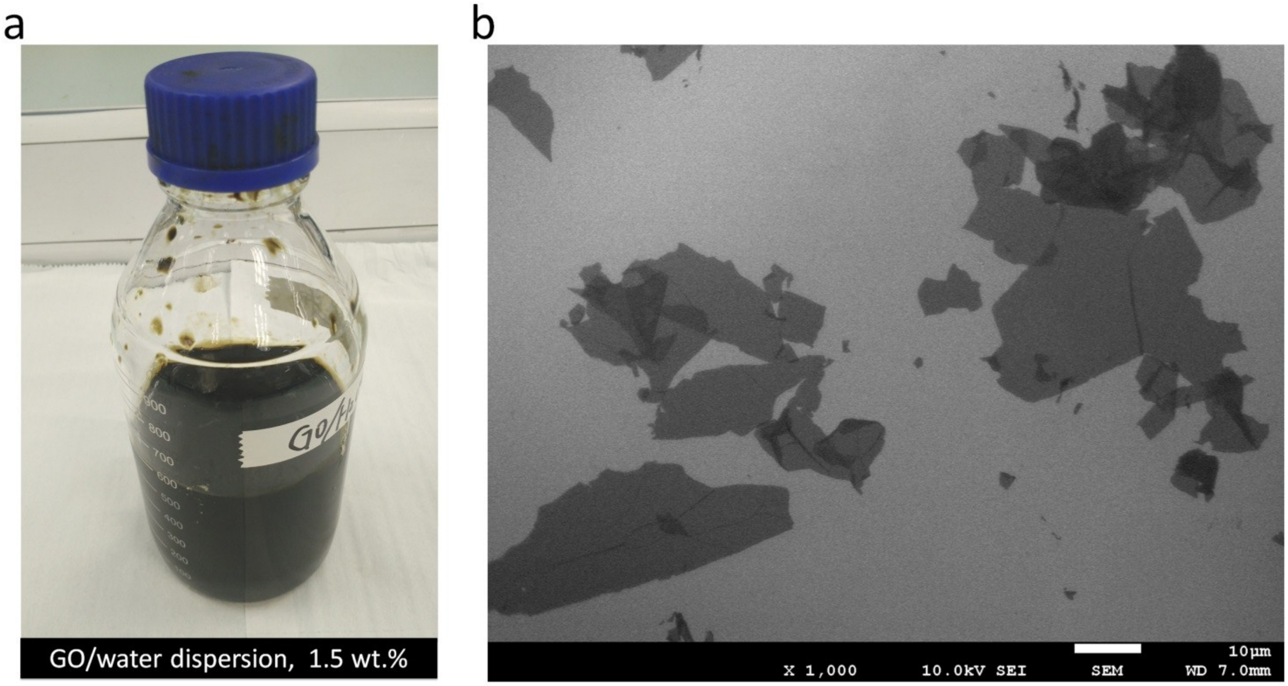

Fig. S1. The GO used in this work. (a) Photograph of GO/water dispersion (1.5 wt.%). (b) SEM of GO sheets on silicon substrate.

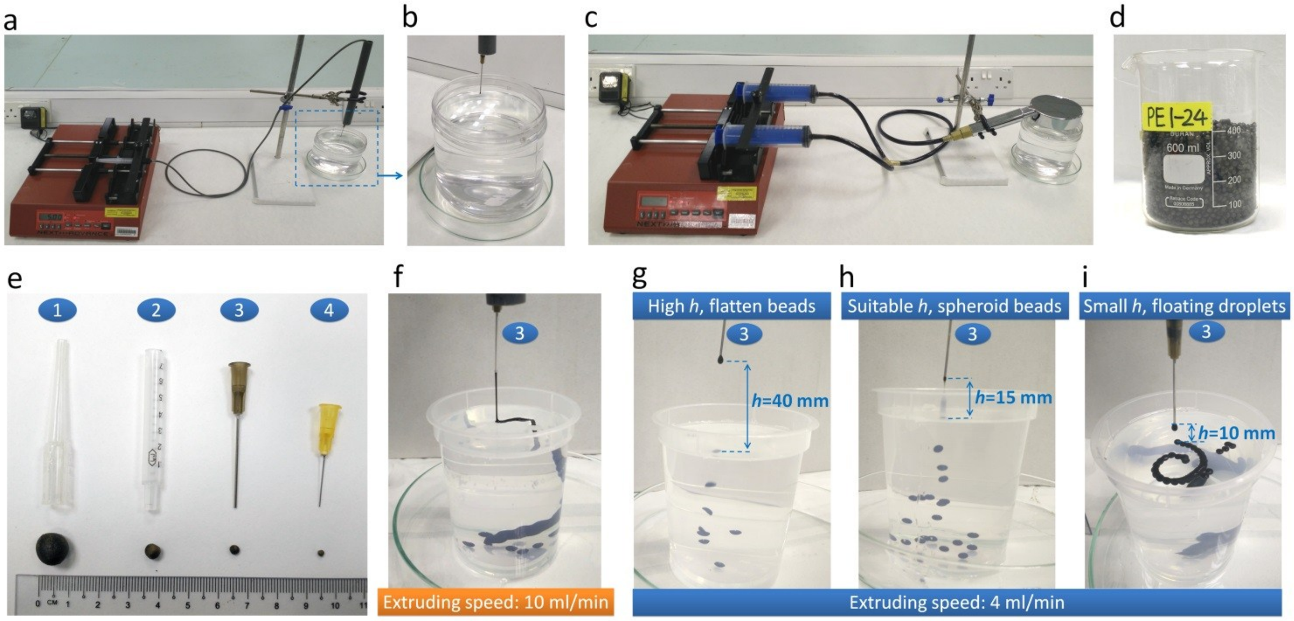

Fig. S2. Preparation of GO beads. (a) A single bead preparation setup, using a needle as nozzle. (b) The needle. (c) A multiple beads preparation setup. (d) GO beads made from 300 mL GO/water dispersion (1.5 wt.%) using the setup in (c) within 10 min. (e) GO beads prepared using nozzles with different diameters. The diameter of the nozzle determines the dimensions of GO beads. (f) Extruding GO/water dispersions at a speed of 10 ml/min, leading to GO fibers. (g–h) Extruding GO/water dispersions at 4 ml/min, leading to GO beads. The nozzle-bath distance, *h*, directly affects the morphology of GO beads, and also the immersion of GO/water droplets.

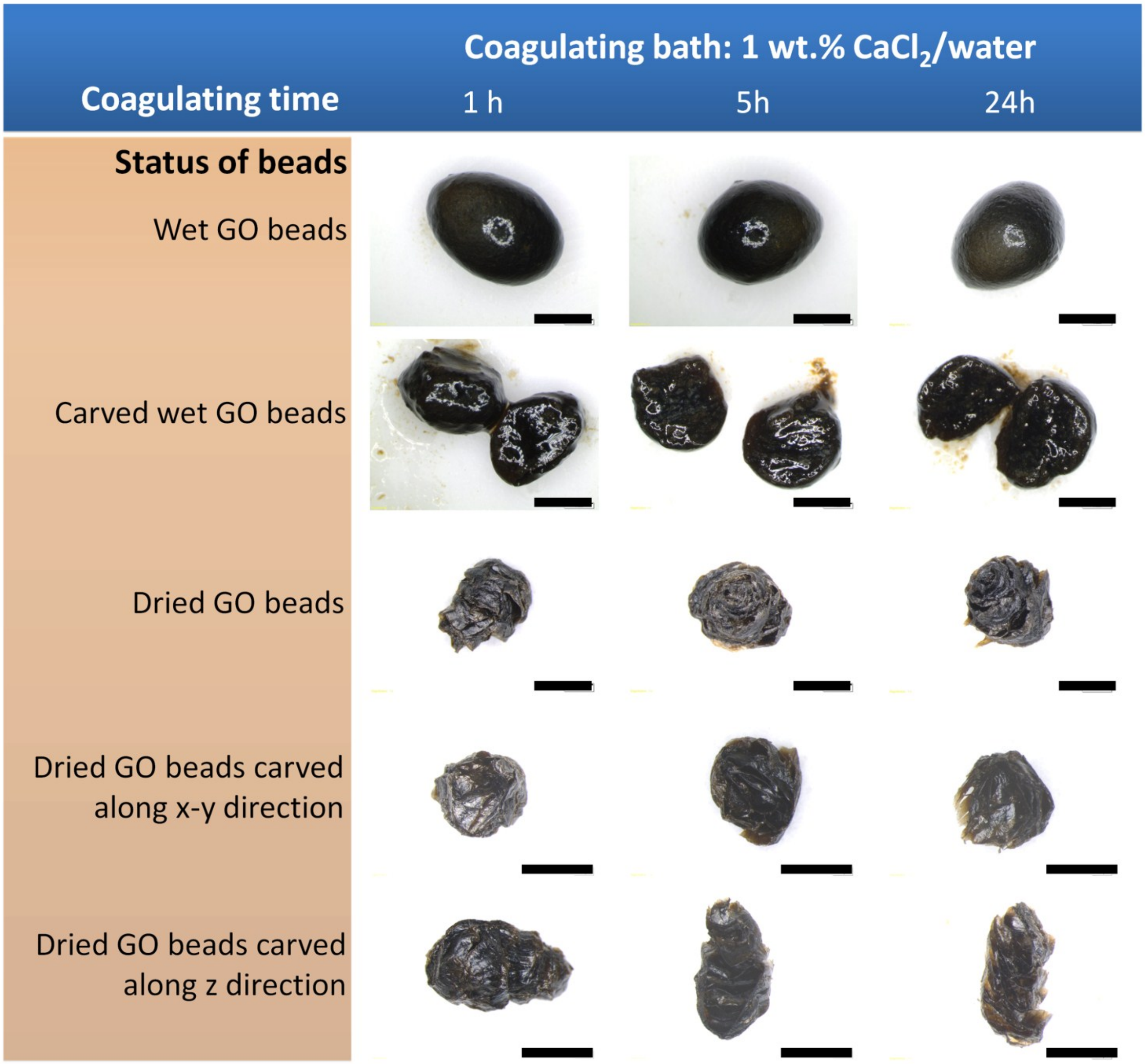

Fig. S3. Optical microscope images of the GO beads coagulated using 1 wt.% $CaCl_2$/water bath. Scale bars 2 mm.

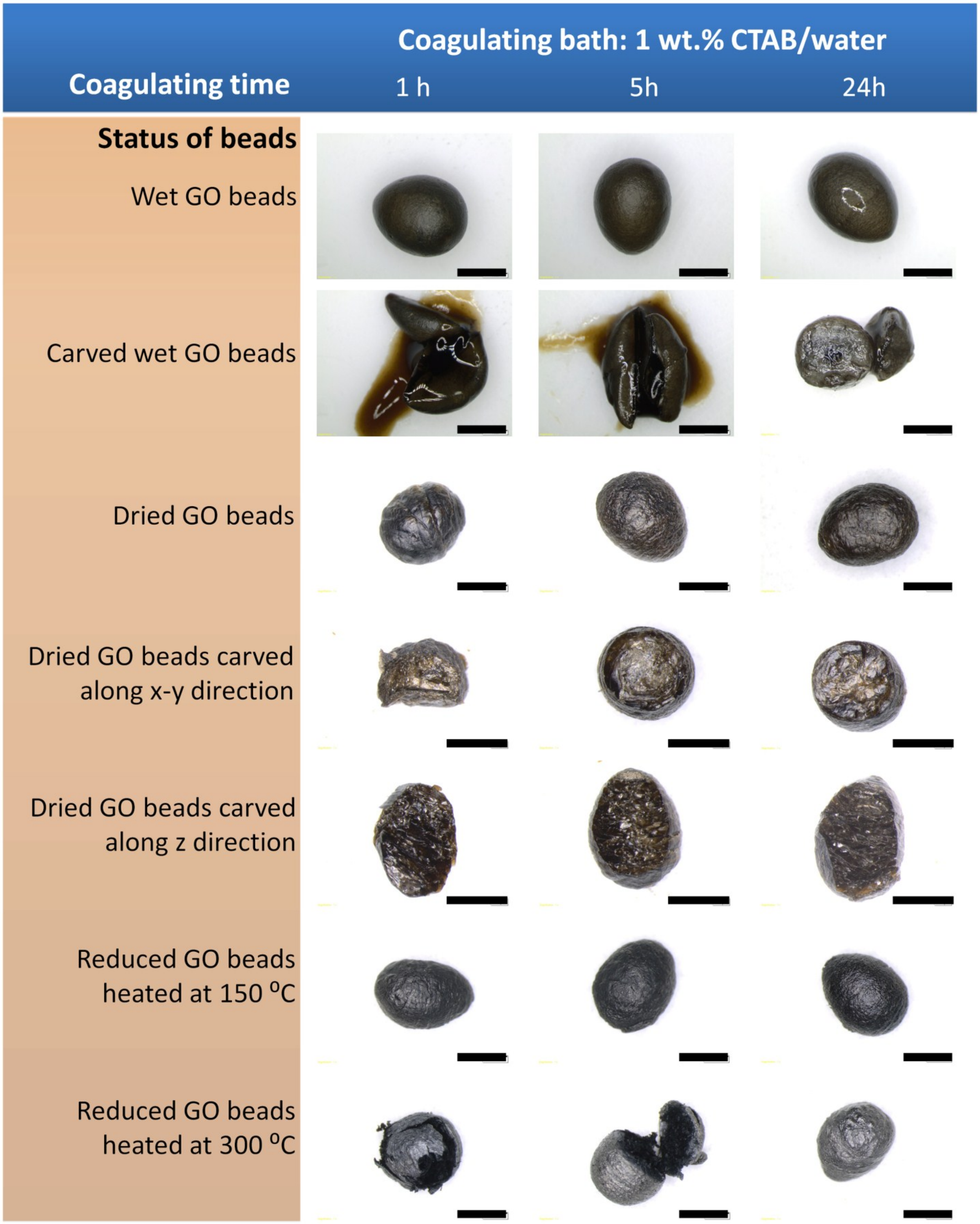

Fig. S4. Optical microscope images of the GO beads coagulated using 1 wt.% CTAB/water bath. Scale bars 2 mm.

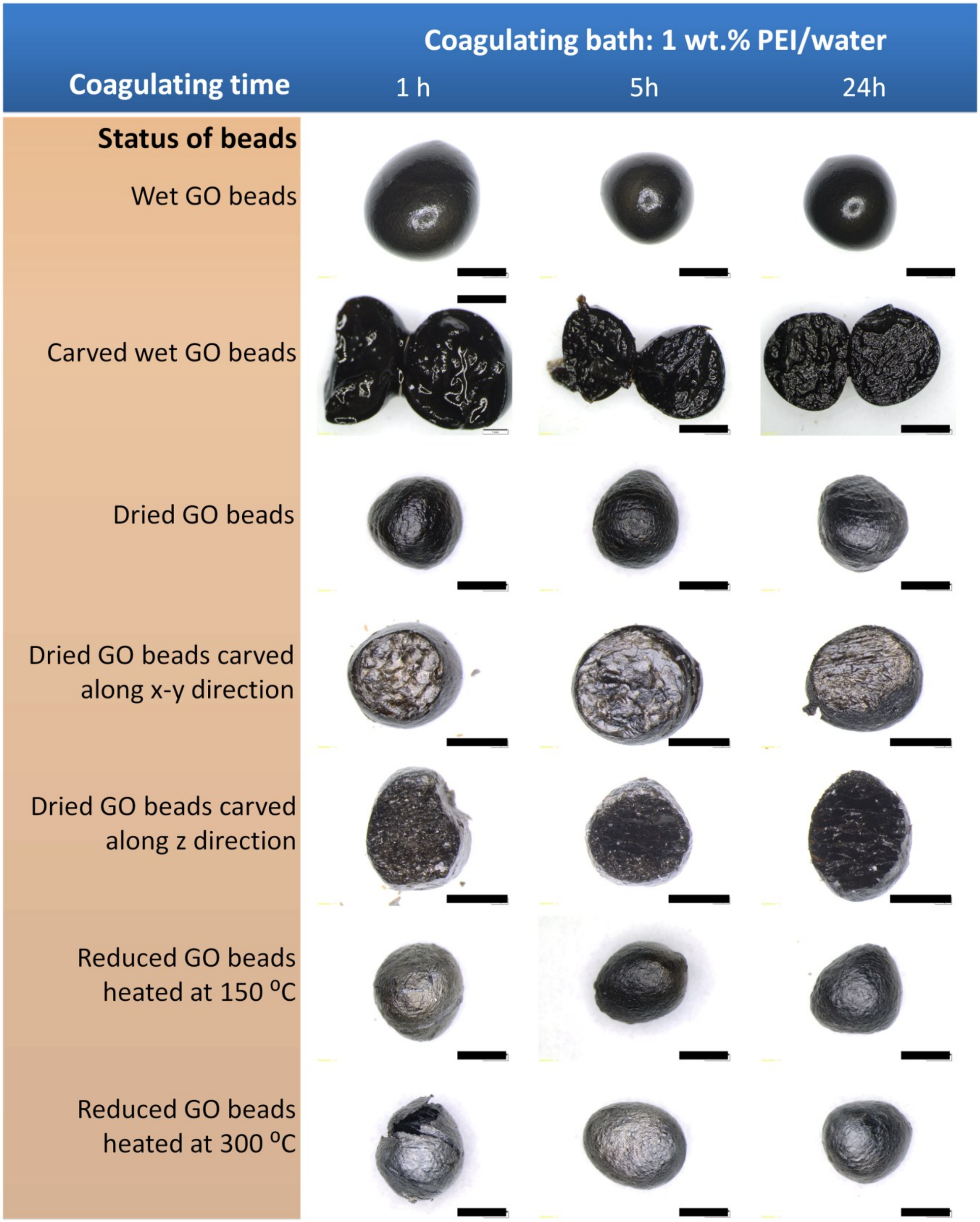

Fig. S5. Optical microscope images of the GO beads coagulated using 1 wt.% PEI/water bath. Scale bars 2 mm.

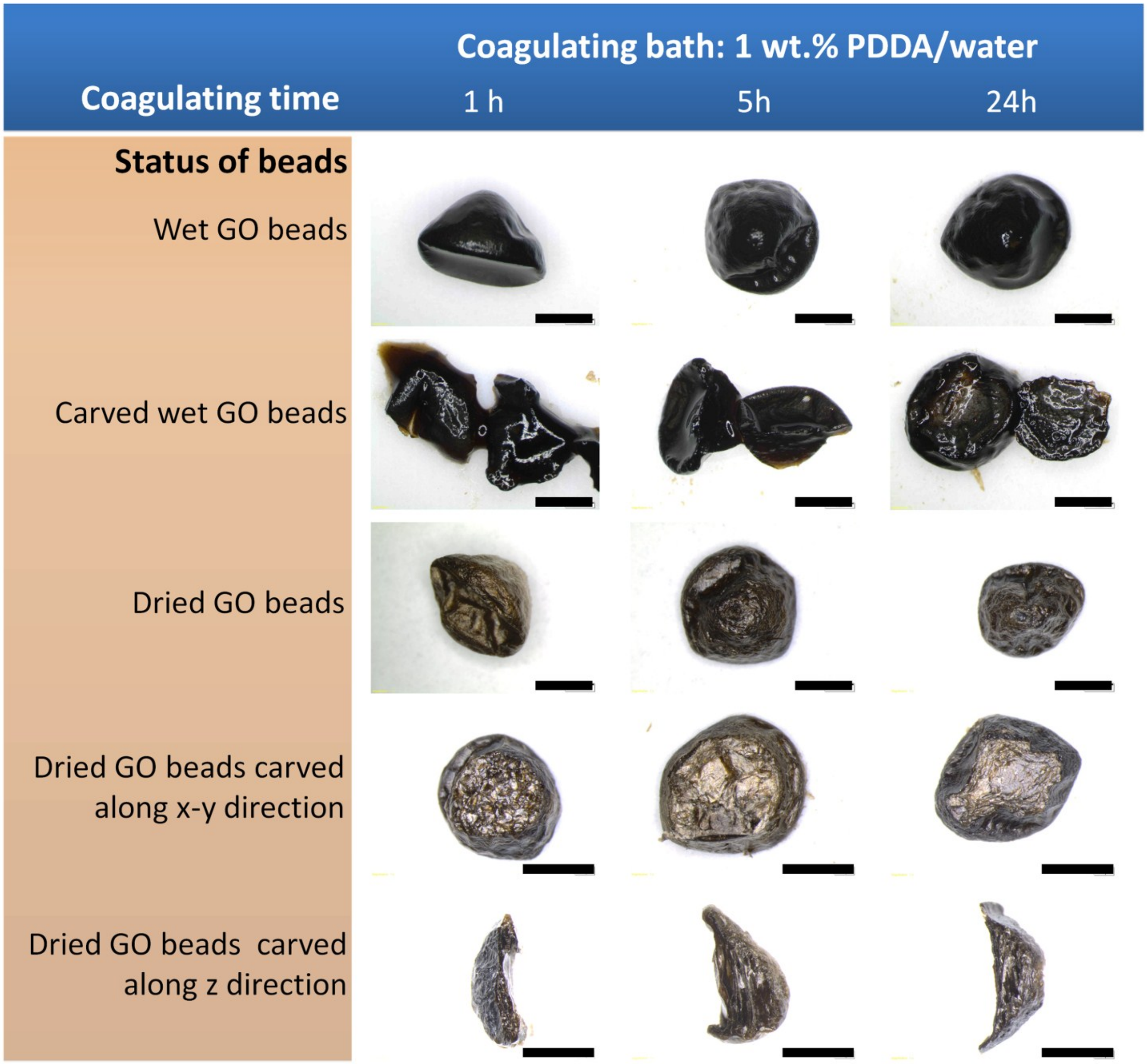

Fig. S6. Optical microscope images of the GO beads coagulated using 1 wt.% PDDA/water bath. Scale bars 2 mm.

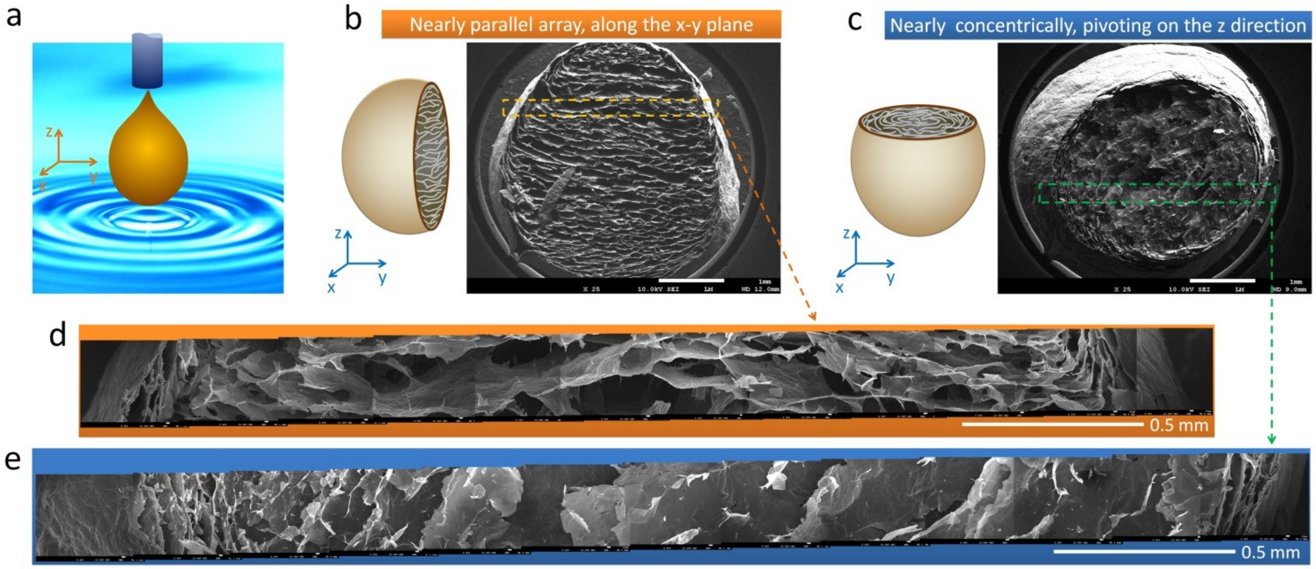

Fig. S7. Micro structures of GO beads PEI-24 h-150 °C. (a) Coordinate axis is designed according to the dripping direction of GO/water droplets. (b, c) SEM images of the cross sections of a typical bead. The inner cores present anisotropic porous structures. GO sheets mostly order along the x-y plane. (d, e) Enlarged sections in (b) and (c), respectively. The broad images are spliced from high magnification SEM images (Fig. S8 and S9).

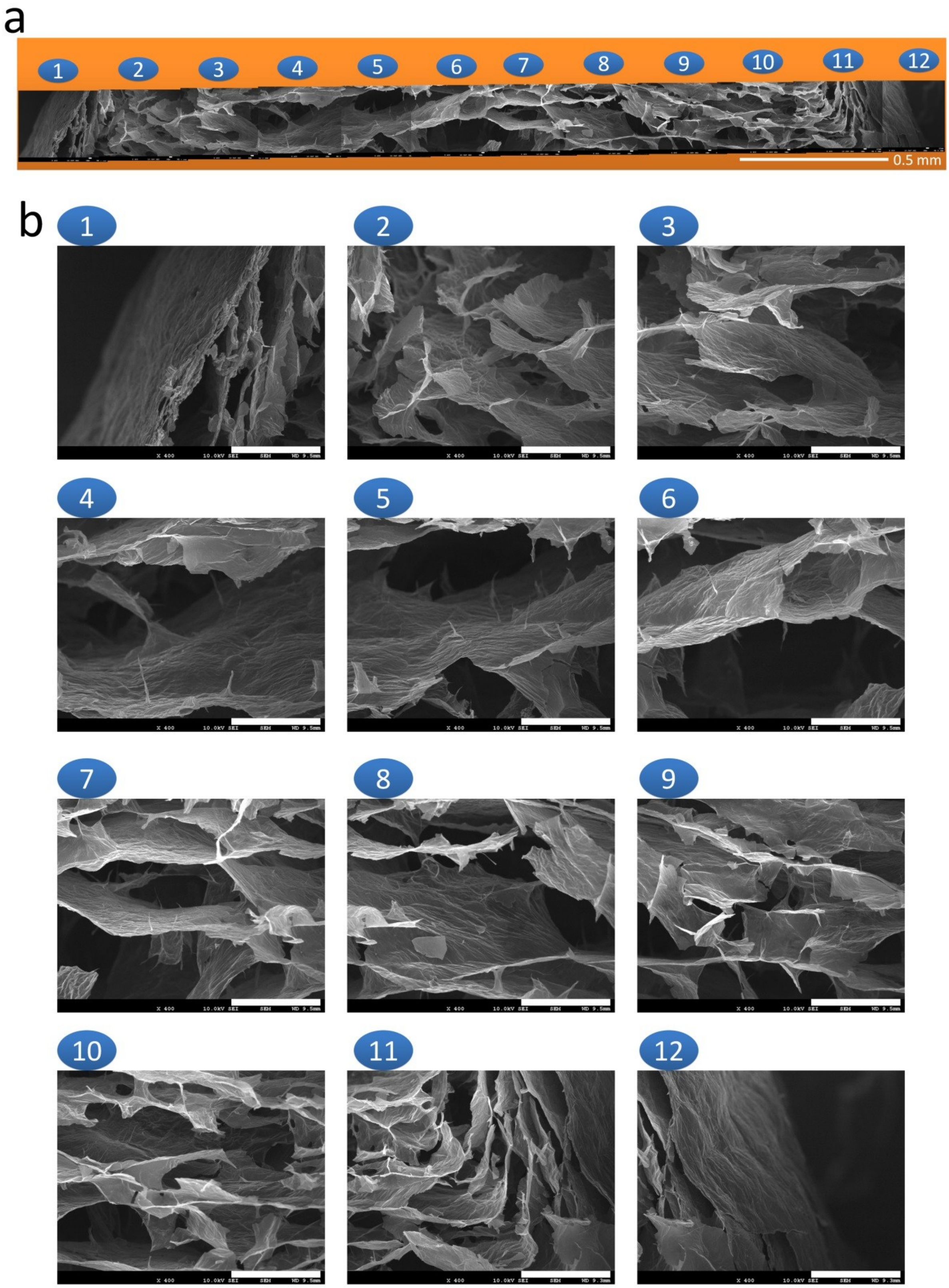

Fig. S8. SEM images with high resolution for the images in Fig. S3. (a) The SEM image in Fig. S7d. (b) The high resolution images. Scale bars 100 µm.

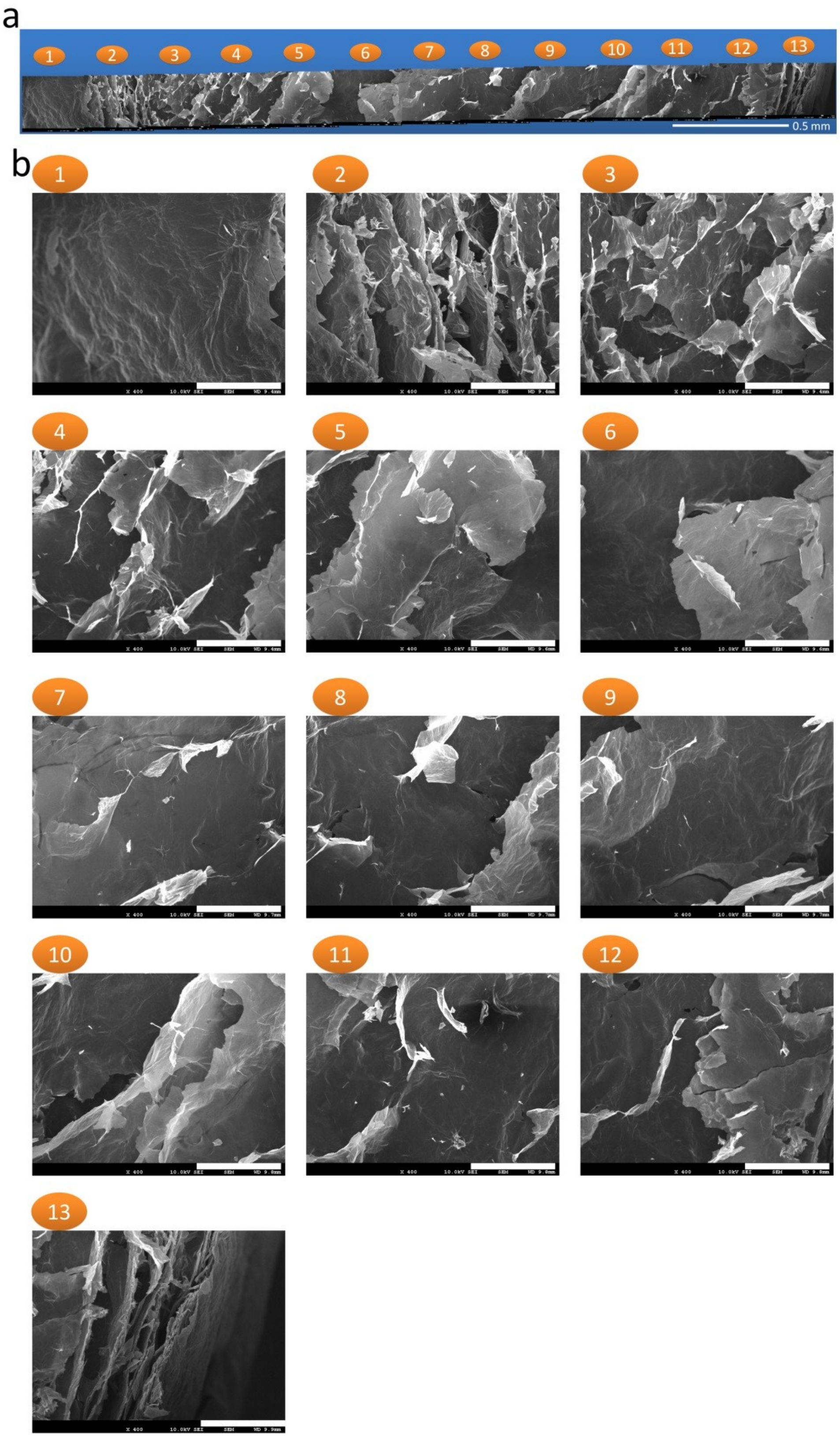

Fig. S9. SEM images with high resolution for the images in Fig. S3. (a) The SEM image in Fig. S7e. (b) The high resolution images. Scale bars 100 µm.

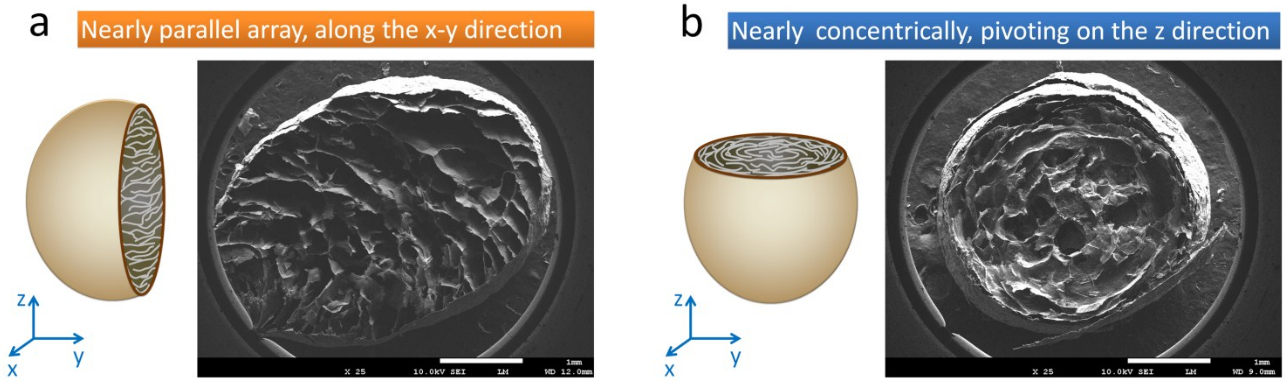

Fig. S10. SEM images of GO beads CTAB-5 h-150 °C. (a) The cross section parallel to z direction. (b) The cross section perpendicular to z direction. Scale bars 1mm.

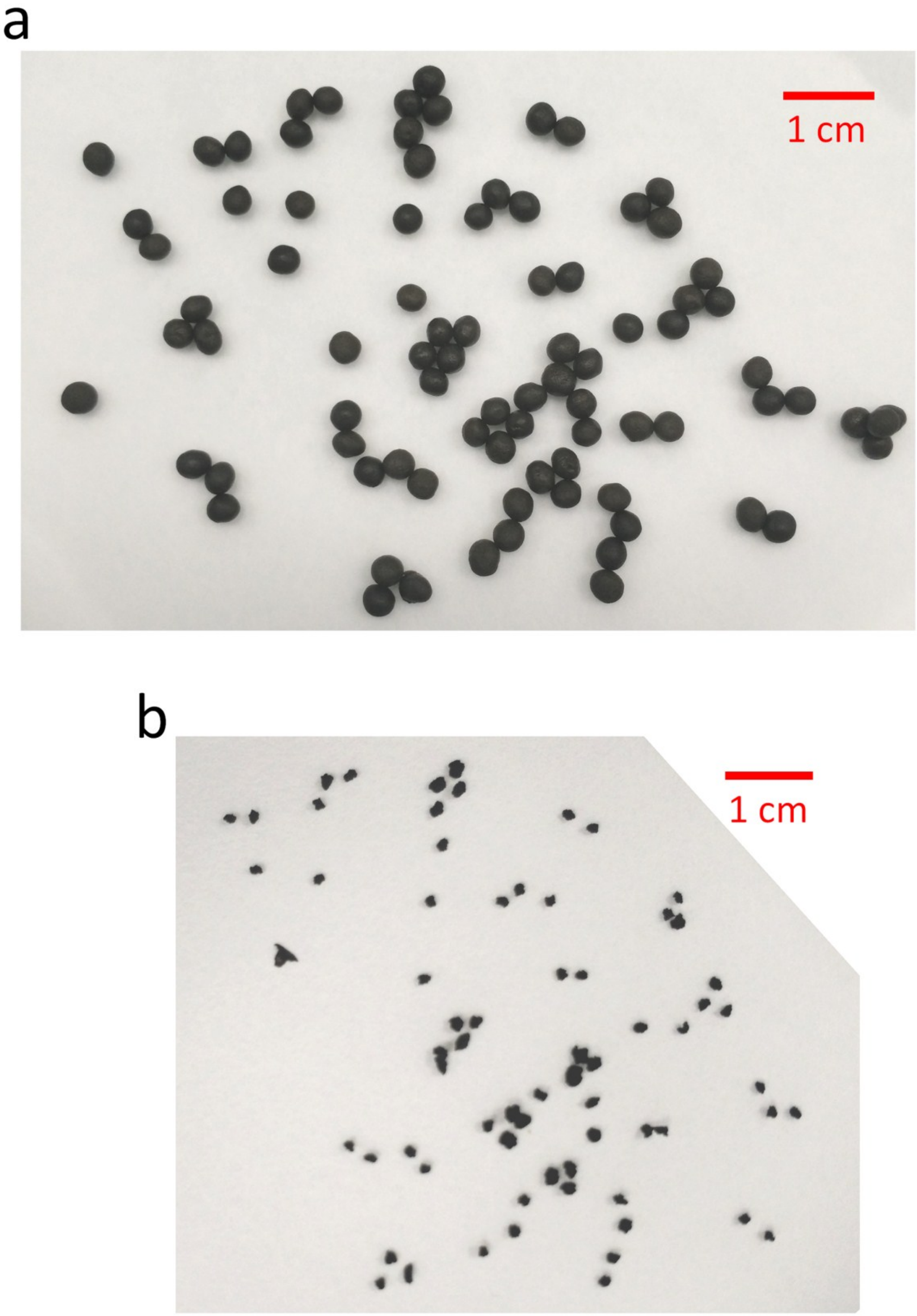

Fig. S11. GO beads (a) before and (b) after dried in a blast oven at 80 °C for 30 min. Obvious shrinkage occurred due to the loss of water from the core of beads.

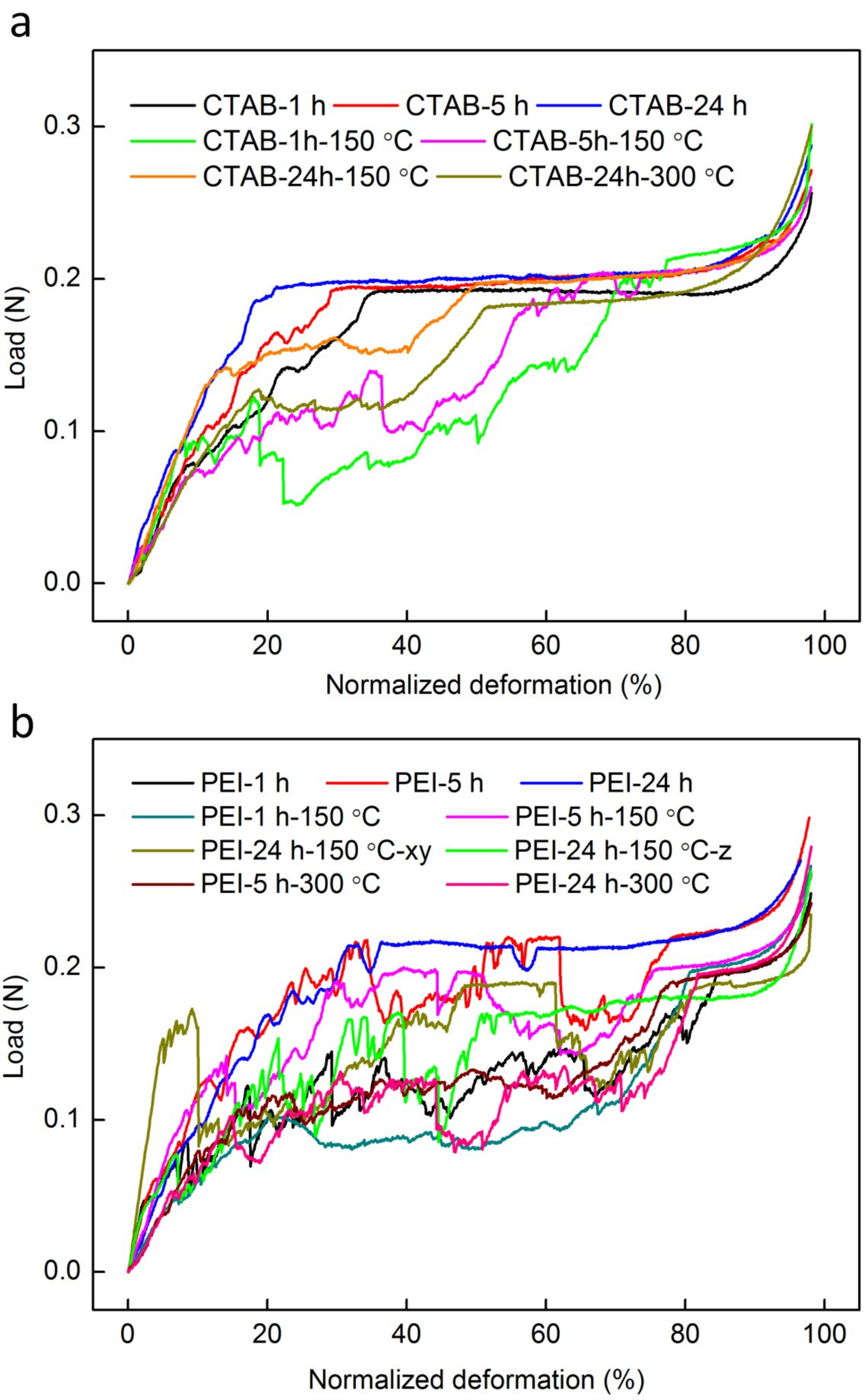

Fig. S12. Compression testing results of GO beads. (a) GO beads coagulated using CTAB bath. (b) GO beads coagulated using PEI bath.

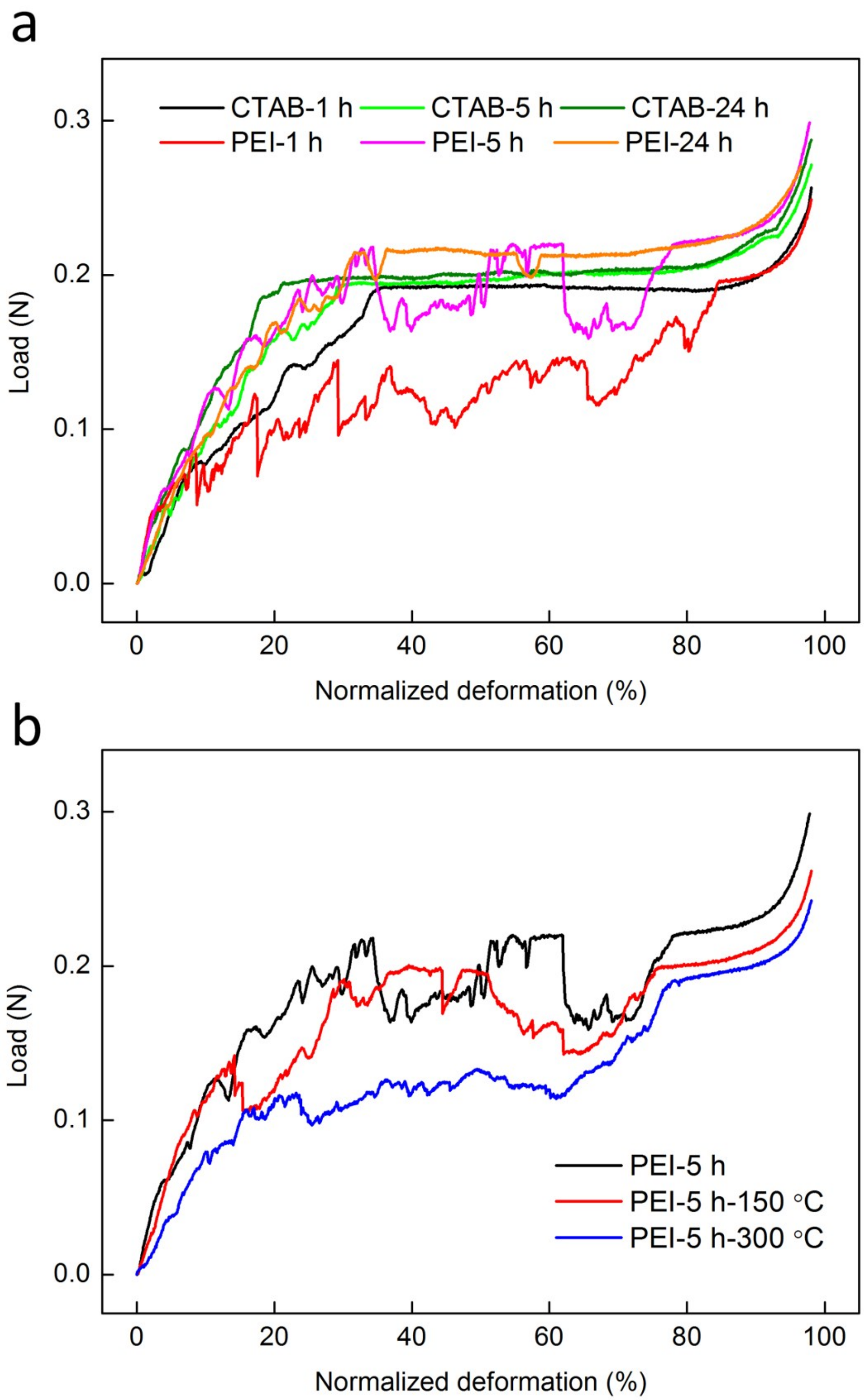

Fig. S13. Comparison between the compress properties of GO beads. (a) The GO beads coagulated in 1 wt.% PEI/water bath is more fragile than the GO beads coagulated using 1 wt.% CTAB/water bath, probably due to the reduction of GO caused by the ammine in PEI. (b) Comparison between the GO beads reduced at different temperatures.

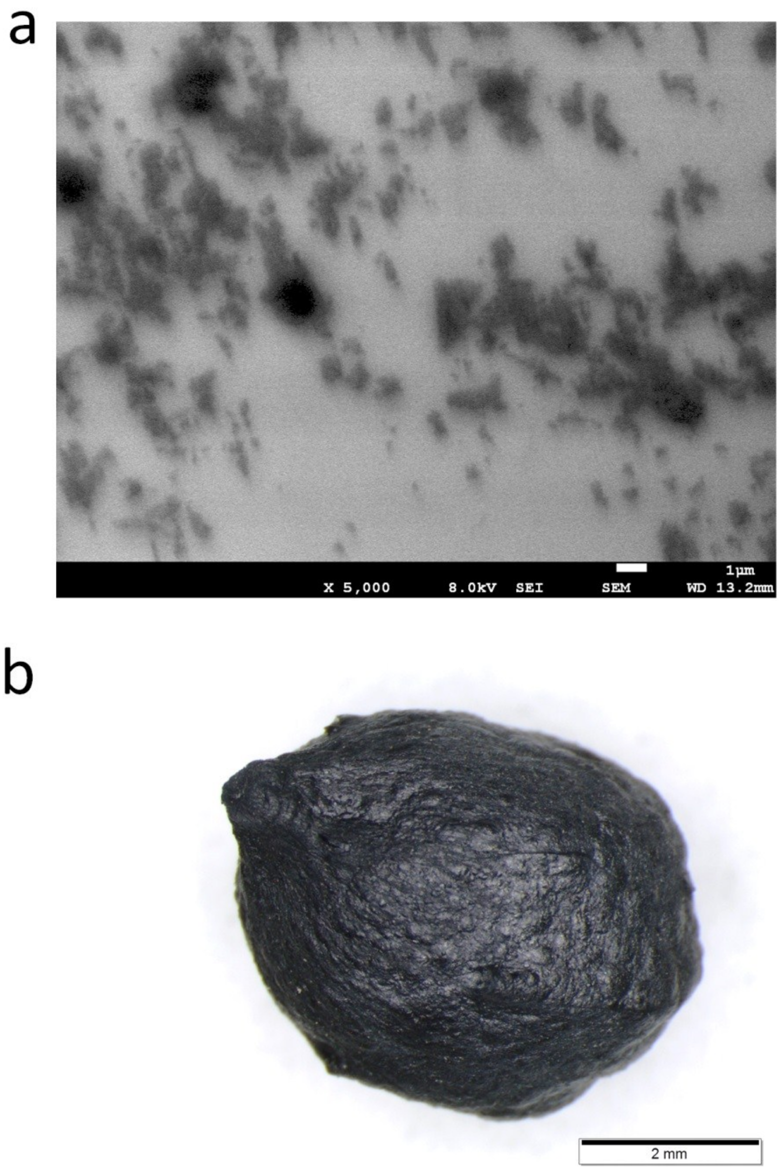

Fig. S14. (a) SEM images of MMT. (b) Optical microscope of a MMT/GO bead.

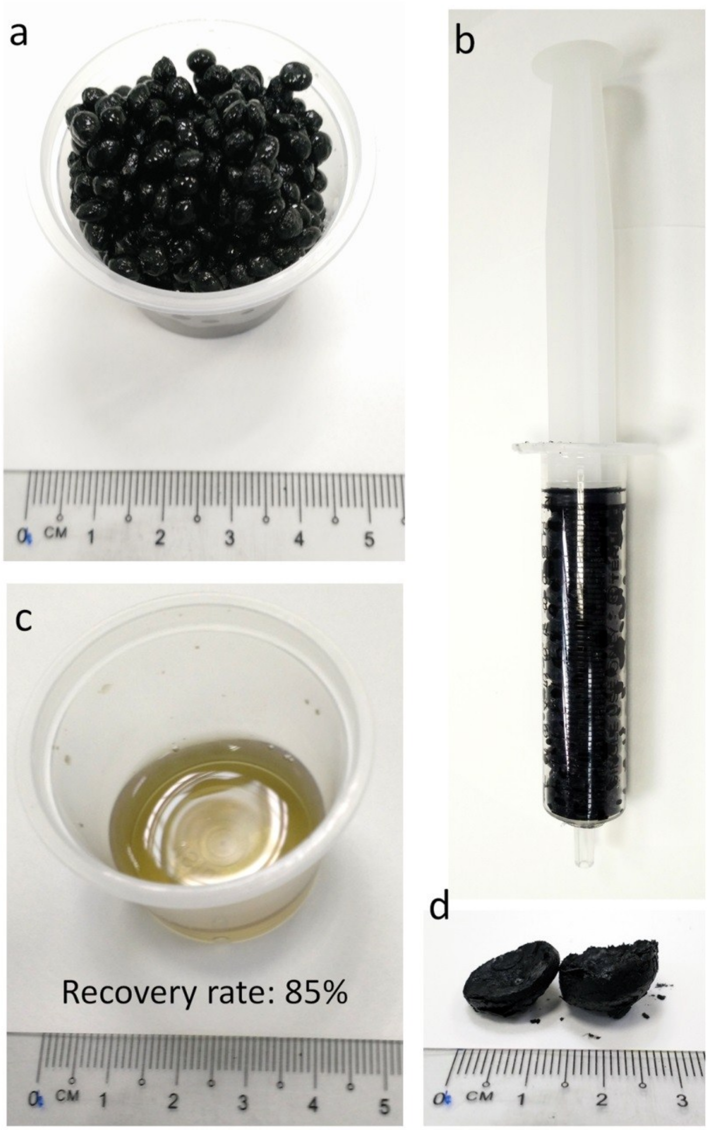

Fig. S15. Recovery of sulfuric acid by squeezing GO beads. (a) GO beads after absorbing concentrated sulfuric acid for 10 min. (b) The GO beads were squeezed using a syringe. (c) The collected sulfuric acid. About 85% of the absorbed sulfuric acid was recovered. (d) The GO beads after squeezing, which were compressed tightly and could not recover to spherical beads.

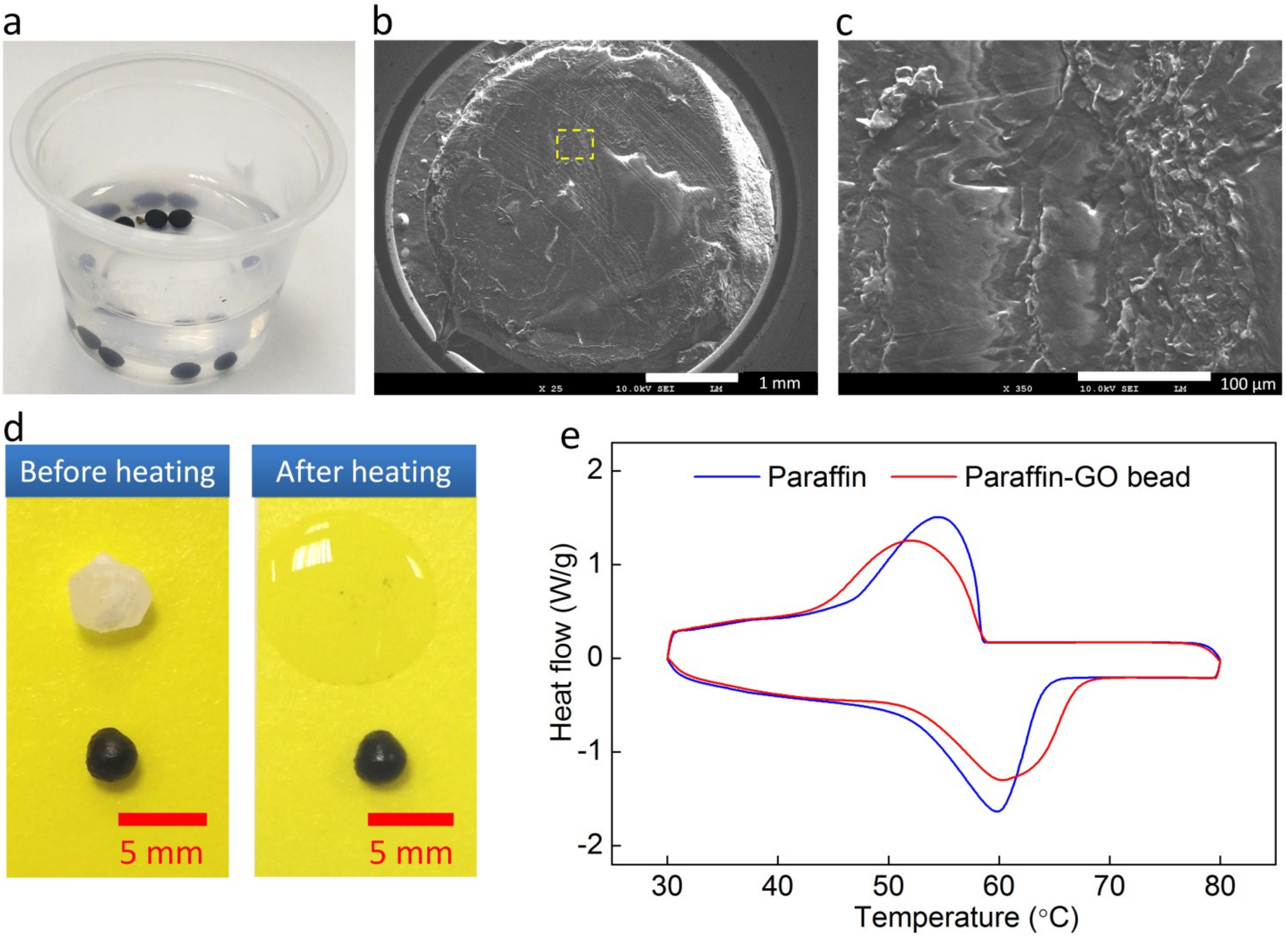

Fig. S16. GO beads for thermal energy storage applications. (a) GO beads depositing in melted paraffin. (b) SEM of the cross section of a paraffin-GO bead. (c) Enlarged area in the yellow frame in (b). (d) GO beads endow paraffin stable shape during heating and cooling cycles. (e) DSC curves of neat paraffin and paraffin-GO beads.

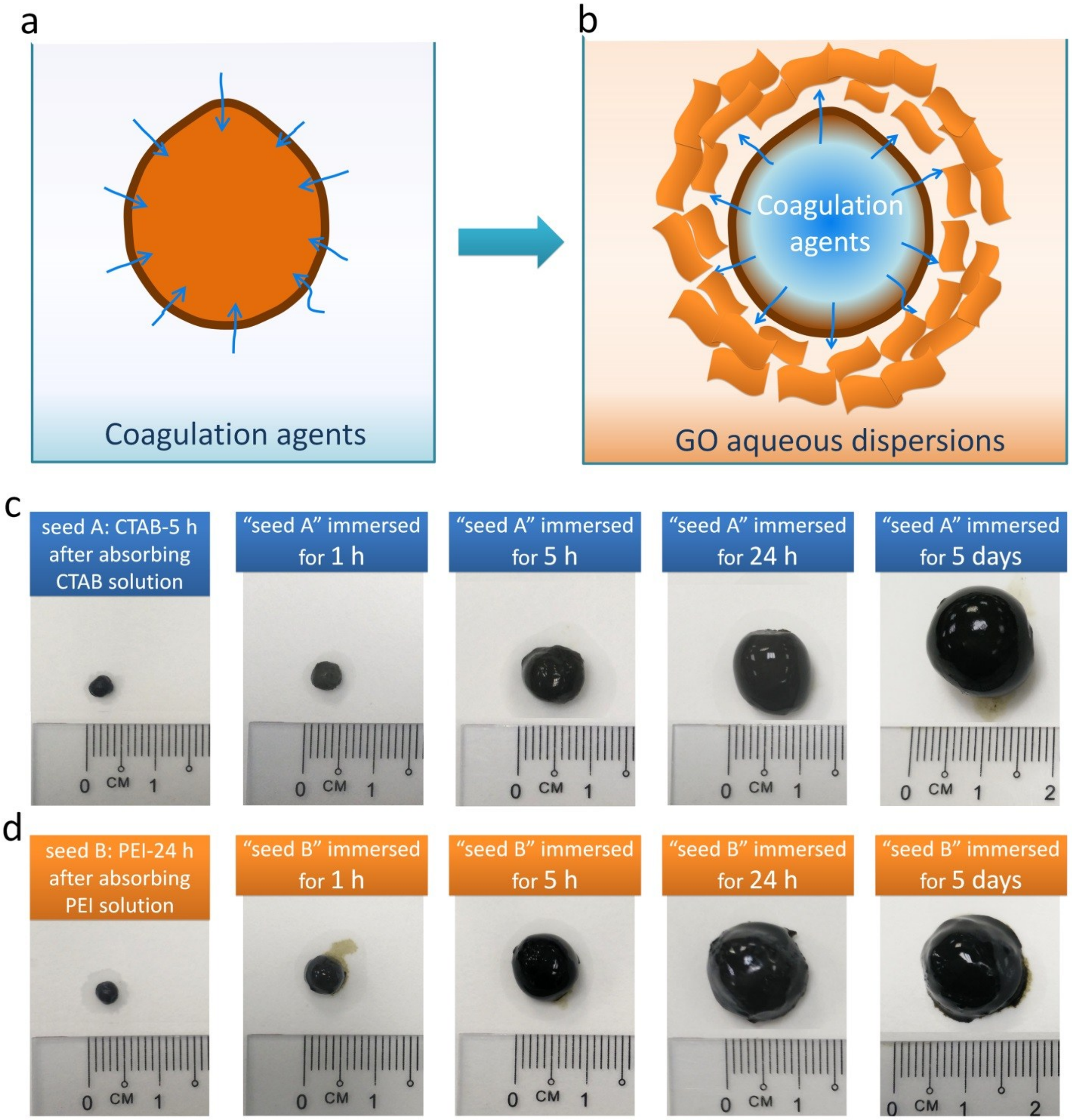

Fig. S17. Extended growth of GO beads. (a) GO beads absorb high concentration coagulation bath. (b) The beads after absorption are immersed in GO aqueous dispersions. The coagulating agents, the CTAB in "seed A" or the PEI in "seed B", diffused into GO/water dispersions slowly, coagulated GO sheets around the "seeds", and thus cause continuous "extended growth". (c) Photographs of "GO beads growth" by placing "seed A" in GO/water dispersions with a variety of time. (d) Photographs of the "GO beads growth" using "seed B".